Advances in Energy and Materials Research
https://jaem.qom.ac.ir/

Bio-synthesis of Pd and Ag nanoparticles supported on celestine and their catalytic performance for reduction of Cr(VI) and methyl orange

Akbar Rostami-Vartooni[1] and Mohammad Yazdian

1. Correspinding authoer, Department of Chemistry, Faculty of Science, University of Qom, Qom, Iran. Email: a.rostami@qom.ac.ir
2. Department of Chemistry, Faculty of Science, University of Qom, Qom, Iran.

Article Info

Article type:
Research Article

Article history:
Received 11 Jun 2024
Received in revised form 17 Sep 2024
Accepted 1 Nov 2024
Published online 25 Dec 2024

Keywords:
Plant extract; Metal nanoparticles; Inorganic support; Celestine; Nanocomposite.

ABSTRACT

This study reports the green synthesis of palladium (Pd) and silver (Ag) nanoparticles (NPs) supported on celestine using an aqueous extract of Amaranthus caudatus flowers as both a reducing and stabilizing agent. The synthesized nanocomposites were characterized by Fourier-transform infrared spectroscopy (FTIR), X-ray diffraction (XRD), field-emission scanning electron microscopy (FESEM), and energy-dispersive X-ray spectroscopy (EDS), revealing well-dispersed spherical Pd and Ag NPs with average sizes below 60 nm anchored on the celestine surface. The nanocomposites demonstrated excellent catalytic activity and reusability in the reduction of Cr(VI) ions (using formic acid) and methyl orange (MO) azo dye (using $NaBH_4$). Notably, Pd NPs/celestine achieved complete reduction of a 10 ppm MO solution in just 30 s, outperforming Ag NPs/celestine (90 s), indicating superior electron transfer efficiency from $NaBH_4$ to MO molecules. These findings highlight the potential of Pd-based catalysts for efficient pollutant degradation.

Cite this article: Rostami-Vartooni, A. & Yazdian, M. (2024). Bio-synthesis of pd and ag nanoparticles supported on celestine and their catalytic performance for reduction of cr(vi) and methyl orange, *Advances in Energy and Materials Research*, *1* (4), 1-7. https://doi.org/10.22091/jaem.2025.11880.1017

DOI: 10.22091/jaem.2025.11880.1017
Publisher: University of Qom.

1. Introduction

Azo dyes and hexavalent chromium (Cr(VI)) have been acknowledged as the most critical and strategic contaminants in water and wastewater, originating from industrial processes [1-3]. These substances pose significant threats to human and animal health due to their carcinogenic and mutagenic properties. Various approaches, including adsorption, photodegradation, chemical reduction, coagulation, ion exchange, and membrane separation, have been employed to effectively eliminate pollutants from wastewater systems [4–8]. Reduction/decolorization process, utilizing $NaBH_4$ or HCOOH as reducing agents, converts hazardous materials into less toxic organic or inorganic compounds [9-11].

Recently, the usage of Ag and Pd nanoparticles (NPs) because of their high specific surface area, chemical stability, and suitable catalytic activity in different chemical reactions such as arylation of phenols, coupling reactions, synthesis of heterocycles, and reduction of toxic azo dyes have been significantly studied [12-16]. Since metal NPs are prone to aggregate, immobilizing them on the surface of different supports such as bentonite, zeolite, perlite, kaolin, graphene oxide, Fe_3O_4, ZrO_2, and CuO leads to their higher reactivity and facile reusability [17-20]. In this field, celestine (or celestite) ore can be used as a support due to its chemical and thermal stability.

The biosynthetic route employing plant extracts for the synthesis of metal NPs offers several advantages, including simplicity, elimination of toxic compounds, lower processing temperatures, and improved control over particle size [21,22]. Flavonoids and non-flavonoids polyphenols in different organs of plants can effectively reduce the metal ions and stabilize the formed NPs [23,24].

Amaranthus Caudatus as an important source of phenolic compounds, has several pharmaceutical activities such as anticancer, antibacterial, anthelmintic, antipyretic, antinociceptive, antidiabetic, antiallergenic, cardioprotective, and hepatoprotective properties [25-27].

In the present work, Pd and Ag NPs were immobilized onto the surface of celestine ore using *A. Caudatus* flower extract. Biosynthesized nanocomposites were used as catalysts to reduce Cr(VI) ions or methyl orange (MO) azo dye from water.

2. Experimental

The celestine ore has the following chemical composition (in %): SrO, 54.57; SO_3, 42.14; CaO, 1.03; SiO_2, 0.23; MgO, 0.32; Na_2O, 0.01; K_2O, 0.04; Al_2O_3, 0.01; Fe_2O_3, 0.09 and TiO_2, 0.01. This natural strontium sulfate was provided from the Koohsefid area in Qom, Iran. The flowers of the *A. Caudatus* plants were collected from the city of Kamu in the Isfahan province of Iran. $AgNO_3$ and $PdCl_2$ were purchased from Aldrich. The concentration of Cr(VI) and MO solutions was monitored using a Lambda-35 UV–Vis spectrophotometer. FTIR spectra of celestine and its Pd and Ag nanocomposites were recorded using a Cary 630 FTIR spectrometer. The X-ray diffraction (XRD) patterns were obtained by a Philips PW 1730 X-ray diffractometer (CuKa = 1.5406). FESEM-EDAX analysis of prepared nanocomposites was performed on the Cam Scan MV2300.

2.1. Preparation of A. Caudatus flower extract

A 250 mL beaker containing 10 g of the dried *A. Caudatus* flowers and 120 mL distilled water was heated at 40 ºC for 20 min. The obtained extract was filtered and applied for the synthesis of Pd and Ag NPs in the following steps.

2.2. Preparation of Pd NPs/Celestine nanocomposite

1 g of celestine was dispersed in 25 mL of *A. Caudatus* extract at ambient temperature using a mechanical stirrer. Subsequently, a solution containing 0.1 g $PdCl_2$ dissolved in 7 mL acetonitrile was added to the mixture and then heated at 50 ºC. Following 30 minutes, the resulting Pd NPs/Celestine nanocomposite was thoroughly rinsed with distilled water and subjected to drying at ambient temperature.

2.3. Preparation of Ag NPs/Celestine nanocomposite

80 mL of *A. Caudatus* flower extract was added to a mixture of celestine ore (1g) dispersed in $AgNO_3$ solution (25 mL, 0.1 M). Then, this mixture was stirred continuously for 30 min at 50 ºC. The obtained Ag/Celestine nanocomposite was washed twice with distilled water and subsequently dried at ambient temperature.

2.4 Catalytic reduction of Cr(VI) ion or MO azo dye using prepared nanocomposites

The celestine and its Pd and Ag nanocomposites (8 mg) were dispersed in 3.4 mM Cr(VI) solution containing 1 mL 88% formic acid as a reducing agent. Also, 8 mg of these catalysts were applied for the reduction of the MO solution (25 mL, 10 ppm) by utilizing the newly prepared $NaBH_4$ solution (25 mL, 5.3×10^{-3} or 10.6×10^{-3} M). The changes in the Cr(VI) and MO concentration were monitored using UV-Vis analysis at λ_{max} of 350 and 465 nm, respectively.

3. Results and discussion

3.1. Preparation of Pd and Ag NPs

As depicted in Scheme 1, the aqueous flower extract of *A. Caudatus* contains various water-soluble phytochemicals, such as flavones and terpenoids, which can undergo enol-form into the keto-form conversion (tautomeric transformations) and subsequently reduce metal ions**.** Additionally, these compounds play an important role as stabilizing agents

due to their hydroxyl and carbonyl functional groups for the synthesized Pd and Ag NPs [28].

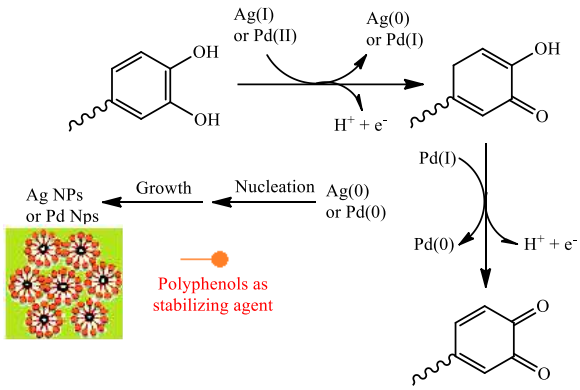

Scheme 1. The plausible mechanism of Ag and Pd NPs preparation in the presence of the plant extract.

3.2. Characterization of the prepared catalysts

The FT-IR spectra of the prepared celestine, Ag NPs/Celestine, and Pd NPs/Celestine are presented in Figure 1. The observed bands at approximately 1090–1200 and 610-640 cm^{-1} are assigned to the SO_4^{2-} bands [29, 30]. The peaks around 1400–1650 cm^{-1} in Figures 1b and 1c are related to the constituents of *A. Caudatus* extract that has been absorbed on the Pd and Ag NPs surfaces as stabilizing agents [31]. The broad peaks at wavenumbers 3800–4500 cm^{-1} can be attributed to O–H stretching vibrations [32,33].

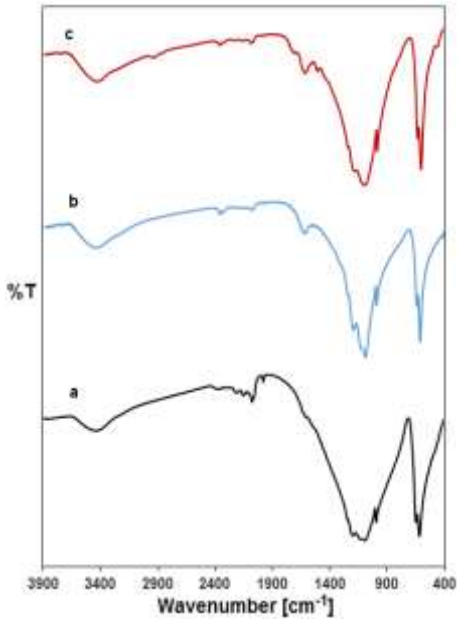

Figure 1. FT-IR spectra of (a) celestine, (b) Ag NPs/Celestine, and (c) Pd NPs/Celestine.

The crystalline structures of the celestine and its synthesized Pd and Ag nanocomposites were evaluated using XRD analysis (Figure 2). The observed diffraction peaks at about 2θ values of 27.1, 28.1, 30.1, 32.8, and 44.3° can be ascribed to the (021), (210), (121), (211), and (212) planes for celestine [34]. The peaks at 2θ values of 37.3 and 44.1 in Figure 2b can be attributed to the (111) and (200) crystal planes of Ag NPs with a face-centered cubic structure (JCPDS card No-87-0719), respectively [35]. In the XRD pattern of Pd/Celestine (Figure 2c), no specific peaks related to the Pd phase are found, possibly due to the high dispersion of the Pd NPs stabilized on the support surface or their amorphous phase [36].

The FESEM images of Pd NPs/Celestine and Ag NPs/Celestine (Figures 3 and 4) indicate the well-dispersed spherical Pd and Ag NPs prepared by the plant extract on the celestine support. Furthermore, the EDS spectra of these nanocomposites confirm the presence of Pd and Ag elements.

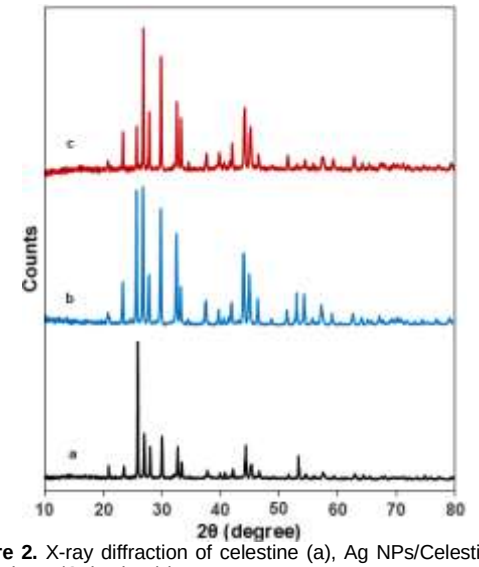

Figure 2. X-ray diffraction of celestine (a), Ag NPs/Celestine (b), and Pd NPs/Celestine (c).

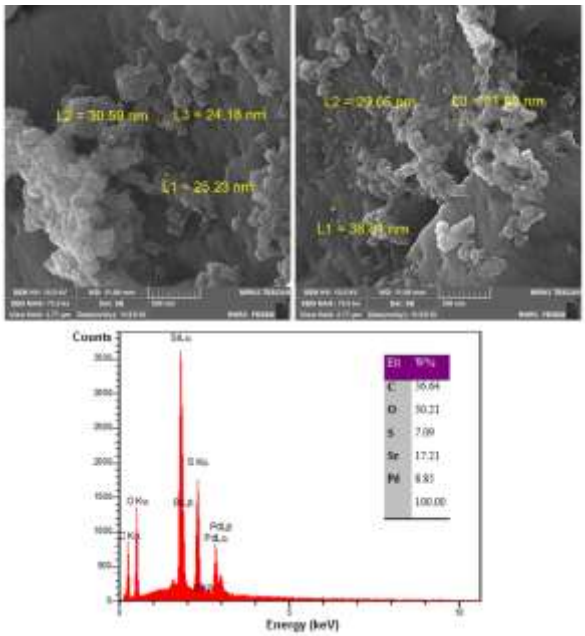

Figure 3. FESEM images and EDS spectrum of the Pd NPs/Celestine nanocomposite.

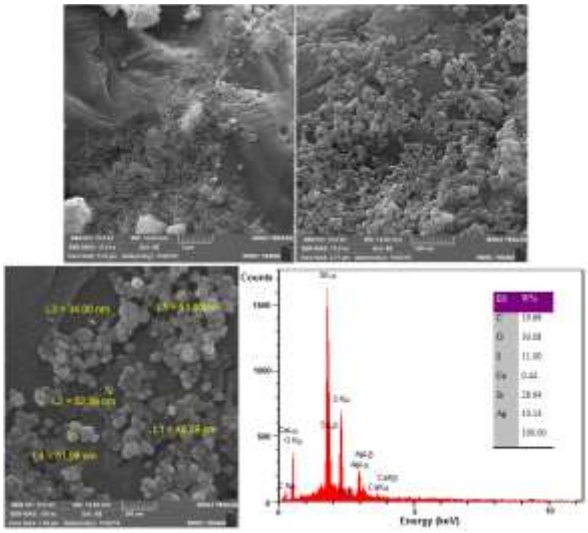

Figure 4. FESEM images and EDS spectrum of the Ag NPs/Celestine nanocomposite.

3.3. Catalytic activity of the Pd NPs/Celestine and Ag NPs/Celestine catalysts for the MO and Cr(VI) reduction

The development of heterogeneous catalysts with exceptional activity in the degradation of pollutants has presented a significant role in the field of environmental applications [37-39]. In this study, the effectiveness of the Ag NPs/Celestine and Pd NPs/Celestine catalysts was evaluated in the reduction/decolorization of the Cr(VI) ion and MO dye as representative pollutants (Scheme 2). The alterations of absorption bands in the UV-Vis spectra of MO and Cr(VI) solutions in the catalytic reductions using Pd NPs/Celestine are depicted in Figure 5a and Figure 5b, respectively. The reduction time of the 3.4 mM Cr(VI) solution containing 1 mL of 88% formic acid using Pd NPs/Celestine was 25 min. However, a significant reduction of Cr(VI) solution was not observed within 60 min using Ag NPs/Celestine. Additionally, the reduction times of the MO solution (10 ppm) were 30 and 90 s in the presence of Pd NPs/celestine and Ag NPs/Celestine catalysts, respectively. The observed results suggest that Pd NPs are more effective than Ag NPs in the electron transfer from reducing agents ($NaBH_4$ or formic acid) to the selected pollutants [28].

Scheme 2. Green synthesis of Pd and Ag NPs supported on celestine and their catalytic investigation in the reduction/decolorization of MO and Cr(VI).

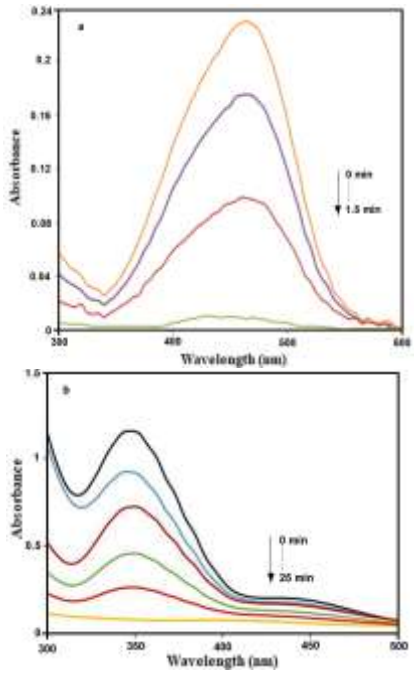

Figure 5. UV-Vis spectra changes of MO (a) and Cr(VI) (b) during the catalytic reduction.

3.4. Recycling of catalyst

Here, the recycling of Pd NPs/Celestine and Ag NPs/Celestine nanocomposites for the MO reduction was investigated. The FESEM images and EDS spectra of the recycled catalysts after four times are shown in Figures 6 and 7. The results show that the Pd and Ag NPs amounts and their morphology have not significantly changed. Hence, there is only a slight decrease in the catalytic activity of recycled nanocomposites due to their good stability and reusability. The MO reaction time in the presence of the recycled Pd NPs/Celestine and Ag NPs/Celestine was about 30 and 100 s, respectively.

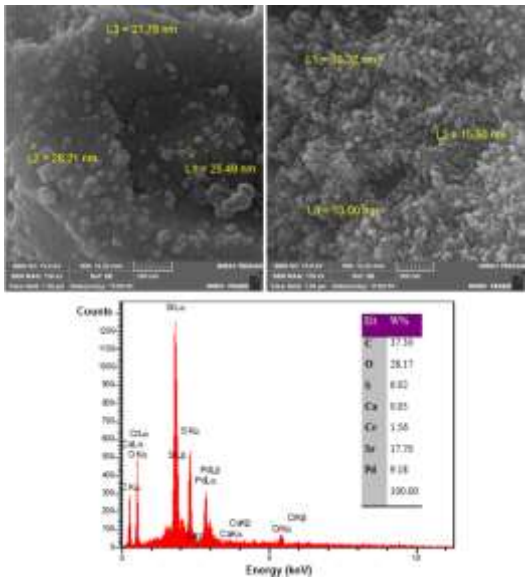

Figure 6. FESEM images and EDS spectrum of the recycled Pd NPs/Celestine nanocomposite.

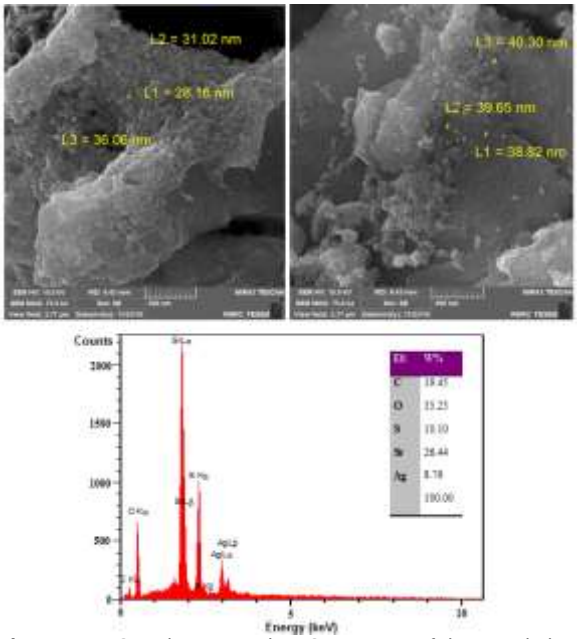

Figure 7. FESEM images and EDS spectrum of the recycled Ag NPs/Celestine nanocomposite.

4. Conclusions

This study successfully synthesized palladium (Pd) and silver (Ag) nanoparticles (NPs) supported on celestine using a green approach with *Amaranthus caudatus* extract as both reducing and stabilizing agent. Comprehensive characterization (FTIR, XRD, EDS, FESEM) confirmed the formation of well-dispersed spherical Pd and Ag NPs (<60 nm) on the celestine surface. The Pd NPs/celestine nanocomposite exhibited superior catalytic activity over its Ag counterpart in the reduction of methyl orange (MO) and Cr(VI), achieving complete decolorization of MO in just 30 s and reduction of Cr(VI) within 25 min using $NaBH_4$ and formic acid, respectively. Notably, both catalysts retained high stability and reusability over four consecutive cycles, with no significant loss in activity. These findings underscore the potential of Pd NPs/celestine as an efficient and sustainable nanocatalyst for environmental remediation of toxic pollutants.

Conflict of Interests

The authors declare no conflicts of interest.

Acknowledgements

The authors gratefully acknowledge the financial support of the University of Qom.

References

[1] M. Maham, M. Nasrollahzadeh, M. Bagherzadeh, R. Akbari, Green synthesis of Palladium/Titanium dioxide nanoparticles and their application for the reduction of methyl orange, congo red and rhodamine B in aqueous medium, Comb. Chem. High Throughput Screen 20(9) (2017) 787–795. https://doi.org/10.2174/1386207320666171023154523.

[2] S. Ghattavi, A. Nezamzadeh-Ejhieh, GC-MASS detection of methyl orange degradation intermediates by AgBr/g-C_3N_4: Experimental design, bandgap study, and characterization of the catalyst, Inter. J. Hydrogen Energy 45 (2020) 24636–24656. https://doi.org/10.1016/j.ijhydene.2020.06.207

[3] C. Chen, K. Zhu, K. Chen, A. Alsaedi, T. Hayat, Synthesis of Ag nanoparticles decoration on magnetic carbonized polydopamine nanospheres for effective catalytic reduction of Cr(VI), J. Colloid Interface Sci. 526 (2018) 1–8. https://doi.org/10.1016/j.jcis.2018.04.094

[4] S.E. Mousavi Ghahfarokhi, N. Alirezaei Varnosfaderani, M. Zargar Shoushtari, The role of Pb and annealing temperature on the structural, magnetic, optical and dielectric properties of W-type hexaferrite nanostructures, Ceram. Int. 44 (2018)17592–17601. https://doi.org/10.1016/j.ceramint.2018.06.018

[5] H. Karimi-Maleh, S. Ranjbari, B. Tanhaei, A. Ayati, Y. Orooji, M. Alizadeh, F. Karimi, S. Salmanpour, J. Rouhi, M. Sillanpää, F. Sen, Novel 1-butyl-3-methylimidazolium bromide impregnated chitosan hydrogel beads nanostructure as an efficient nanobio-adsorbent for cationic dye removal: Kinetic study, Environ. Res. 195 (2021)110809. https://doi.org/10.1016/j.envres.2021.110809

[6] E.M. Sahin, T. Tongur, E. Ayranci, Removal of azo dyes from aqueous solutions by adsorption and electrosorption as monitored with in-situ UV-visible spectroscopy, Sep. Sci. Technol. 55 (2020) 3287–3298. https://doi.org/10.1080/01496395.2019.1676786

[7] K. Pakzad, H. Alinezhad, M. Nasrollahzadeh, Green synthesis of Ni@Fe_3O_4 and CuO nanoparticles using *Euphorbia maculata* extract as photocatalysts for the degradation of organic pollutants under UV-irradiation, Ceram. Int. 45(14) (2019) 17173-17182. https://doi.org/10.1016/j.ceramint.2019.05.272

[8] A. Rajan, C. Yazhini, M.D. Dhileepan, B. Neppolian, Leveraging the photocatalytic Cr (VI) reduction by an IRMOF-3@NH_2-MIL-101 (Fe) heterostructure based on interfacial Lewis acid-base interaction, Chemosphere 352 (2024) 141473. https://doi.org/10.1016/j.chemosphere.2024.141473

[9] M. Nasrollahzadeh, Z. Issaabadi, S.M. Sajadi, Green synthesis of Pd/Fe_3O_4 nanocomposite using *Hibiscus tiliaceus* L. extract and its application for reductive catalysis of Cr(VI) and nitro compounds, Sep. Purif. Technol. 197 (2018) 253–260. https://doi.org/10.1016/j.seppur.2018.01.010

[10] A. Rostami-Vartooni, Green synthesis of CuO nanoparticles loaded on the seashell surface using *Rumex crispus* seeds extract and its catalytic applications for reduction of dyes, IET nanobiotechnol. 11 (2017) 349–359. https://doi.org/10.1049/iet-nbt.2016.0149

[11] K. Li, J. Zho, F. Zhang, Morphology-controlled fabrication of Nb^{5+} doped $SrTiO_3$ for promoting photocatalytic reduction of Cr(VI), Molecular Catalysis 553 (2024) 113754. https://doi.org/10.1016/j.mcat.2023.113754

[12] A. Rostami-Vartooni, A. Moradi-Saadatmand, M. Mahdavi, Catalytic reduction of organic pollutants using biosynthesized Ag/C/Fe_3O_4 nanocomposite by red water and Caesalpinia gilliesii flower extract, Mater. Chem. Phys. 219 (2018) 328–339. https://doi.org/10.1016/j.matchemphys.2018.08.026

[13] M. Nasrollahzadeh, M. Maham, A. Rostami-Vartooni, M. Bagherzadeh, S.M. Sajadi, Barberry fruit extract assisted in situ green synthesis of Cu nanoparticles supported on a reduced graphene oxide–Fe_3O_4 nanocomposite as a magnetically separable and reusable catalyst for the O-arylation of phenols with aryl halides under ligand-free conditions, RSC Adv. 5(79) (2015) 64769–64780. https://doi.org/10.1039/C5RA10037B

[14] A. Rostami-Vartooni, M. Alizadeh, M. Bagherzadeh, Green synthesis characterization and catalytic activity of natural bentonite-supported copper nanoparticles for the solvent-free synthesis of 1-substituted 1*H*-1,2,3,4-tetrazoles and reduction of 4-nitrophenol, Beilstein. J. Nanotech. 6 (2015) 2300–2309. https://doi.org/10.3762/bjnano.6.236

[15] R. Bayan, N. Karak, Photo-assisted synthesis of a Pd–Ag@CQD nanohybrid and its catalytic efficiency in promoting the Suzuki–Miyaura cross-coupling reaction under ligand-free and ambient conditions, ACS Omega 12 (2017) 8868-8876. https://doi.org/10.1021/acsomega.7b01504

[16] P. Verma, Y. Kuwahara, K. Mori, H. Yamashita, Pd/Ag and Pd/Au bimetallic nanocatalysts on mesoporous silica for plasmon-mediated enhanced catalytic activity under visible light irradiation, J. Mater. Chem. A. 4 (2016) 10142-10150. https://doi.org/10.1039/C6TA01664B

[17] V. Rocha, S. Franco, A.R. Bertão, I.C. Neves, T. Tavares, Recycling of natural and waste materials as supports for green silver nanoparticles as efficient catalysts in photodegradation of organic pollutants, Environ. Technol. Innov. 34 (2024) 103576. https://doi.org/10.1016/j.eti.2024.103576

[18] M. Navlani-García, M. Martis, D. Lozano-Castelló, D. Cazorla-Amorós, K. Mori, H. Yamashita, Investigation of Pd nanoparticles supported on zeolites for hydrogen production from formic acid dehydrogenation, Catal. Sci. Technol. 5 (2015) 364-371. https://doi.org/10.1039/C4CY00667D

[19] H. Faroughi Niya, N. Hazeri, M. Fatahpour, P. Roudini, M. Shirzaei, Immobilizing Pd nanoparticles on Fe_3O_4@tris (hydroxymethyl) aminomethane MNPs as a novel catalyst for the synthesis of bis (pyrazolyl) methane derivatives, J. Molecular Structure 1239 (2021) 130400. https://doi.org/10.1016/j.molstruc.2021.130400

[20] C. Hu, Z. Chen, C. Wei, X. Wan, W. Li, Q. Lin, Au nanoparticles supported on iron-based oxides for soot oxidation: physicochemical properties before and after the reaction. ACS Omega 6 (2021) 11510−11518. https://doi.org/10.1021/acsomega.1c00619

[21] B. Tahmasebi zade Damirchi, F. Rostami Charati, R. Akbari, A. Daneshvar, Green synthesis of silver nanoparticles using the aqueous extract of Viscum album Fruit, Nanochem. Res. 5(1) (2020) 104-110. https://doi.org/10.22036/ncr.2020.01.010

[22] J. Kadam, S. Madiwale, B. Bashte, S. Dindorkar, P. Dhawal, P. More, Green mediated synthesis of palladium nanoparticles using aqueous leaf extract of *Gymnema sylvestre* for catalytic reduction of Cr (VI), SN Applied Sciences 2 (2020) 1854. https://doi.org/10.1007/s42452-020-03663-5

[23] H. Veisi, B. Karmakar, T. Tamoradi, R. Tayebee, S. Sajjadifar, S. Lotfi, B. Maleki. S. Hemmati, Bio-inspired synthesis of palladium nanoparticles fabricated magnetic Fe_3O_4 nanocomposite over Fritillaria imperialis flower extract as an efficient recyclable catalyst for the reduction of nitroarenes, Scientific Reports 11 (2021) 4515. https://doi.org/10.1038/s41598-021-83854-1

[24] A. Rostami-Vartooni, A. Moradi-Saadatmand, Green synthesis of magnetically recoverable Fe_3O_4 /HZSM-5 and its Ag nanocomposite using *Juglans regia* L. leaf extract and their evaluation as catalysts for reduction of organic pollutants, IET nanobiotechnol. 13 (2019) 407–415. https://doi.org/10.1049/iet-nbt.2018.5089

[25] H. Li, Z. Deng, R. Liu, H. Zhu, J. Draves, M. Marcone, Y. Sun, R. Tsao, Characterization of phenolics, betacyanins and antioxidant activities of the seed, leaf, sprout, flower and stalk extracts of three Amaranthus species, J. Food Compos. Anal. 37 (2015) 75–81. https://doi.org/10.1016/j.jfca.2014.09.003

[26] A.V. Quiroga, D.A. Barrio, M.C. Añón, Amaranth lectin presents potential antitumor properties, LWT-Food Sci. Technol. 60 (2015) 478–485. https://doi.org/10.1016/j.lwt.2014.07.035

[27] A. Martinez-Lopez, M.C. Millan-Linares, N.M. Rodriguez-Martin, F. Millan, S. Montserrat-de la Paz, Nutraceutical value of kiwicha (*Amaranthus caudatus L.*), J. Funct. Foods 65 (2020) 103735. https://doi.org/10.1016/j.jff.2019.103735

[28] A. Rostami-Vartooni, L. Rostami, M. Bagherzadeh, Green synthesis of Fe_3O_4/bentonite-supported Ag and Pd nanoparticles and investigation of their catalytic activities for the reduction of azo dyes, J. Mater. Sci. Mater. Electron 30(24) (2019) 21377–21387. https://doi.org/10.1007/s10854-019-02514-3

[29] D. Bingo, S. Aydogan, S.K. Bozbas, Production of $SrCO_3$ and $(NH_4)_2SO_4$ by the dry mechanochemical processing of celestite, J. Ind. Eng. Chem. 18 (2012) 834–838. https://doi.org/10.1016/j.jiec.2011.11.145

[30] W. Mohamed, S.S. Darweesh, Ancient Egyptian black patinated copper aloys. Archaeometry 53(1) (2012) 175-192. https://doi.org/10.1111/j.1475-4754.2011.00602.x

[31] Á.B. Sifontes, E. Cañizales, J. Toro-Mendoza, E. Ávila, P. Hernández, B.A. Delgado, G.B. Gutiérrez, Y. Díaz, E. Cruz-Barrios, Obtaining highly crystalline barium sulphate nanoparticles via chemical precipitation and quenching in absence of polymer stabilizers, Journal of Nanomaterials (2015) 510376. https://doi.org/10.1155/2015/510376

[32] M.R. Shaik, Z.J.Q. Ali, M. Khan, M. Kuniyil, M.E. Assal, H.Z. Alkhathlan, A. Al-Warthan, M.R.H. Siddiqui, M. Khan, S.F. Adil, Green synthesis and characterization of palladium nanoparticles using *origanum vulgare L.* extract and their catalytic activity, Molecules 22(1) (2017) 165. https://doi.org/10.3390/molecules22010165

[33] M. Tsakiridou, I. Tsagkalias, R.M. Papi, D.S. Achilias, Synthesis of novel nanocomposite materials with eenhanced antimicrobial activity based on poly(ethylene glycol methacrylate)s with Ag, TiO_2 or ZnO nanoparticles, Nanomaterials 14(3) (2024) 291. https://doi.org/10.3390/nano14030291

[34] K. Için, S. Öztürk, S.E. Sünbül, Investigation and characterization of high purity and nano-sized $SrCO_3$ production by mechanochemical synthesis process, Ceram. Int. 47 (2021) 33897-33911. https://doi.org/10.1016/j.ceramint.2021.08.302

[35] A. Rostami-Vartooni, M. Nasrollahzadeh, M. Alizadeh, Green synthesis of perlite supported silver nanoparticles using *Hamamelis virginiana* leaf extract and investigation of its catalytic activity for the reduction of 4-nitrophenol and Congo red, J. Alloys Compd. 680 (2016) 309–314. https://doi.org/10.1016/j.jallcom.2016.04.008

[36] J. Xu, L. Zhu, H. Zhang, X. Deng, K. Li, B.H. Chen, SiO_2-supported Pd nanoparticles for highly efficient, selective and stable phenol hydrogenation to cyclohexanone, Molecular Catalysis, 538 (2023) 112975. https://doi.org/10.1016/j.mcat.2023.112975

[37] M. Nasrollahzadeh, N.S.S. Bidgoli, Z. Issaabadi, Z. Ghavamifar,T. Baran, R. Luque, *Hibiscus Rosasinensis* L. aqueous extract-assisted valorization of lignin: preparation of magnetically reusable Pd NPs@Fe_3O_4-lignin for Cr(VI) reduction and Suzuki-Miyaura reaction in eco-friendly media, J. Biol. Macromol. 148 (2020) 265-275. https://doi.org/10.1016/j.ijbiomac.2020.01.107

[38] M. Nasrollahzadeh, Z. Issaabadi, Reduction of Cr(VI) and 4-nitrophenol in aqueous media using *N*-heterocyclic palladium complex immobilized on the nano Fe_3O_4@SiO_2 as a magnetically recyclable catalyst, Sep. Purif. Technol. 211 (2018) 809-815. https://doi.org/10.1016/j.seppur.2018.10.045

[39] G. Oroumi, A. Hemmatzadeh, K.H. Salem, E.A. Dawi, F. Samimi, G.F. Hameed, Z.A. Taha, M. Salavati-Niasari, Green sol-gel auto-combustion synthesis of CeO_2/$MnCr_2O_4$ nanocomposite using banana juice and its potential application for enhanced degradation of methyl orange under visible light, Alexandria Engineering Journal 102 (2024) 26-35. https://doi.org/10.1016/j.aej.2024.05.109